An explicit formula for metal wire plasmon of terahertz wave

Jie Yang,[1, 2] Qing Cao,[2,*] and Changhe Zhou[1]

[1] *Shanghai Institute of Optics and Fine Mechanics, Chinese Academy of Sciences, 390 Qinghe Road, Jiading District, Shanghai 201800, China*

[2] *Department of Physics, Shanghai University, 99 Shangda Road, Baoshan District, Shanghai 200444, China*

**qcao@shu.edu.cn*

Abstract: An explicit formula for metal wire plasmon of terahertz wave is analytically derived. The derivation is based on the huge relative permittivities of nonmagnetic metals in the spectral region of terahertz wave, some important properties of modified Bessel functions, and a suitable Taylor expansion. The obtained formula is further checked by many numerical tests. We find that, for all 11 tested nonmagnetic metals, for the whole spectral region of terahertz wave, and for the wide radius range from 10 μm to infinity, the relative deviation for the effective index is always smaller than 5%. This good agreement clearly shows that the derived expression can be conveniently used for the analysis and design of metal wire plasmon of terahertz wave.

OCIS Codes: (240.6680) Surface plasmon; (260.3090) Infrared, far; (230.7370) Waveguides; (260.3910) Metal, optics.

References

1. B. B. Hu, and M. C. Nuss, "Imaging with terahertz waves," Opt. Lett. **20**(16), 1716–1718 (1995).
2. A. Nahata, A. S. Weling, and T. F. Heinz, "A wideband coherent terahertz spectroscopy system using optical rectification and electro-optic sampling," Appl. Phys. Lett. **69**(16), 2321 (1996).
3. M. J. Fitch, and R. Osiander, "Terahertz waves for communications and sensing," Johns Hopkins APL Tech. Dig. **25**, 348–355 (2004).
4. K. Wang, and D. M. Mittleman, "Metal wires for terahertz wave guiding," Nature **432**(7015), 376–379 (2004).
5. Q. Cao, and J. Jahns, "Azimuthally polarized surface plasmons as effective terahertz waveguides," Opt. Express **13**(2), 511–518 (2005).
6. M. Walther, M. R. Freeman, and F. A. Hegmann, "Metal-wire terahertz time-domain spectroscopy," Appl. Phys. Lett. **87**(26), 261107 (2005).
7. T.-I. Jeon, J.-Q. Zhang, and D. Grischkowsky, "THz Sommerfeld wave propagation on a single metal wire," Appl. Phys. Lett. **86**(16), 161904 (2005).
8. H. Cao, and A. Nahata, "Coupling of terahertz pulses onto a single metal wire waveguide using milled grooves," Opt. Express **13**(18), 7028–7034 (2005).
9. M. Wächter, M. Nagel, and H. Kurz, "Frequency-dependent characterization of THz Sommerfeld wave propagation on single-wires," Opt. Express **13**(26), 10815–10822 (2005).
10. K. Wang, and D. M. Mittleman, "Guided propagation of terahertz pulses on metal wires," J. Opt. Soc. Am. B **22**(9), 2001–2008 (2005).
11. K. Wang, and D. M. Mittleman, "Dispersion of surface plasmon polaritons on metal wires in the terahertz frequency range," Phys. Rev. Lett. **96**(15), 157401 (2006).
12. J. A. Deibel, K. Wang, M. D. Escarra, and D. M. Mittleman, "Enhanced coupling of terahertz radiation to cylindrical wire waveguides," Opt. Express **14**(1), 279–290 (2006).
13. J. A. Deibel, N. Berndsen, K. Wang, D. M. Mittleman, N. C. J. van der Valk, and P. C. M. Planken, "Frequency-dependent radiation patterns emitted by THz plasmons on finite length cylindrical metal wires," Opt. Express **14**(19), 8772–8778 (2006).
14. Y. Chen, Z. Song, Y. Li, M. Hu, Q. Xing, Z. Zhang, L. Chai, and C. Y. Wang, "Effective surface plasmon polaritons on the metal wire with arrays of subwavelength grooves," Opt. Express **14**(26), 13021–13029 (2006).
15. C. Themistos, B. M. Azizur Rahman, M. Rajarajan, V. Rakocevic, and K. T. V. Grattan, "Finite Element Solutions of Surface-Plasmon Modes in Metal-Clad Dielectric Waveguides at THz Frequency," J. Lightwave Technol. **24**(12), 5111–5118 (2006).

#116803 - $15.00 USD Received 10 Sep 2009; revised 13 Oct 2009; accepted 13 Oct 2009; published 29 Oct 2009

16. X. He, J. Cao, and S. Feng, "Simulation of the Propagation Property of Metal Wires Terahertz Waveguides," Chin. Phys. Lett. **23**(8), 2066–2069 (2006).
17. J. A. Deibel, M. Escarra, N. Berndsen, K. Wang, and D. M. Mittleman, "Finite-Element Method Simulations of Guided Wave Phenomena at Terahertz Frequencies," Proc. IEEE **95**(8), 1624–1640 (2007).
18. H. Liang, S. Ruan, and M. Zhang, "Terahertz surface wave propagation and focusing on conical metal wires," Opt. Express **16**(22), 18241–18248 (2008).
19. Y. B. Ji, E. S. Lee, J. S. Jang, and T.-I. Jeon, "Enhancement of the detection of THz Sommerfeld wave using a conical wire waveguide," Opt. Express **16**(1), 271–278 (2008).
20. P. W. Smorenburg, and W. P. E. M. Op 't Root, and O. J. Luiten, "Direct generation of terahertz surface plasmon polaritons on a wire using electron bunches'," Phys. Rev. B **78**(11), 115415 (2008).
21. J. A. Deibel, K. Wang, M. Escarra, N. Berndsen, and D. M. Mittleman, "The excitation and emission of terahertz surface plasmon polaritons on metal wire waveguides," C. R. Phys. **9**(2), 215–231 (2008).
22. S. P. Jamison, R. W. McGowan, and D. Grischkowsky, "Single-mode waveguide propagation and reshaping of sub-ps terahertz pulses in sapphire fibers," Appl. Phys. Lett. **76**(15), 1987 (2000).
23. H. Han, H. Park, M. Cho, and J. Kim, "Terahertz pulse propagation in a plastic photonic crystal fiber," Appl. Phys. Lett. **80**(15), 2634 (2002).
24. J. Harrington, R. George, P. Pedersen, and E. Mueller, "Hollow polycarbonate waveguides with inner Cu coatings for delivery of terahertz radiation," Opt. Express **12**(21), 5263–5268 (2004).
25. L. J. Chen, H. W. Chen, T. F. Kao, J. Y. Lu, and C. K. Sun, "Low-loss subwavelength plastic fiber for terahertz waveguiding," Opt. Lett. **31**(3), 308–310 (2006).
26. A. Hassani, A. Dupuis, and M. Skorobogatiy, "Porous polymer fibers for low-loss Terahertz guiding," Opt. Express **16**(9), 6340–6351 (2008).
27. G. Ren, Y. Gong, P. Shum, X. Yu, J. Hu, G. Wang, M. Ong Ling Chuen, and V. Paulose, "Low-loss air-core polarization maintaining terahertz fiber," Opt. Express **16**(18), 13593–13598 (2008).
28. S. Atakaramians, S. Afshar V, B. M. Fischer, D. Abbott, and T. M. Monro, "Porous fibers: a novel approach to low loss THz waveguides," Opt. Express **16**(12), 8845–8854 (2008).
29. R. W. McGowan, G. Gallot, and D. Grischkowsky, "Propagation of ultrawideband short pulses of terahertz radiation through submillimeter-diameter circular waveguides," Opt. Lett. **24**(20), 1431–1433 (1999).
30. R. Mendis, and D. Grischkowsky, "Plastic ribbon THz waveguides," J. Appl. Phys. **88**(7), 4449 (2000).
31. G. Gallot, S. P. Jamison, R. W. McGowan, and D. Grischkowsky, "Terahertz waveguides," J. Opt. Soc. Am. B **17**(5), 851–863 (2000).
32. W. Shi, and Y. J. Ding, "Designs of terahertz waveguides for efficient parametric terahertz generation," Appl. Phys. Lett. **82**(25), 4435 (2003).
33. M. Nagel, A. Marchewka, and H. Kurz, "Low-index discontinuity terahertz waveguides," Opt. Express **14**(21), 9944–9954 (2006).
34. M. Wächter, M. Nagel, and H. Kurz, M. L. Nagel, and H. Kurz, "Metallic slit waveguide for dispersion-free low-loss terahertz signal transmission," Appl. Phys. Lett. **90**(6), 061111 (2007).
35. A. Ishikawa, S. Zhang, D. A. Genov, G. Bartal, and X. Zhang, "Deep subwavelength terahertz waveguides using gap magnetic plasmon," Phys. Rev. Lett. **102**(4), 043904 (2009).
36. H. Raether, Surface Plasmons on Smooth and Rough Surfaces and on Gratings, (Springer, Berlin, 1988).
37. M. I. Stockman, "Nanofocusing of optical energy in tapered plasmonic waveguides," Phys. Rev. Lett. **93**(13), 137404 (2004).
38. U. Schröter, and A. Dereux, "Surface plasmon polaritons on metal cylinders with dielectric core," Phys. Rev. B **64**(12), 125420 (2001).
39. M. Born, and E. Wolf, Principles of Optics, 5th ed. (Pergamon Press, Oxford, 1975).
40. M. A. Ordal, R. J. Bell, R. W. Alexander Jr., L. L. Long, and M. R. Querry, "Optical properties of fourteen metals in the infrared and far infrared: Al, Co, Cu, Au, Fe, Pb, Mo, Ni, Pd, Pt, Ag, Ti, V, and W," Appl. Opt. **24**(24), 4493–4499 (1985).

1. Introduction

Terahertz (THz) wave, locating between the infrared and microwave bands in the electromagnetic spectrum, is one of the hot research topics. It is normally defined as the range from 0.1 to 10 THz (or correspondingly, from 30 μm to 3 mm in wavelength). In recent years, terahertz technology has shown potential applications in many fields, such as in sensing, imaging, and spectroscopy [1–3]. Among those research works, effective THz waveguides have attracted more and more interests [4–35]. In 2004, Wang and Mittleman [4] reported that a simple metal wire can effectively guide THz wave. Since then, many interesting theoretical and experimental works on metal wire THz waveguide have been carried out [5–21].

It was quickly shown that the THz waveguide effect of metal wire comes from the azimuthally polarized surface plasmon [5]. The effective index of this kind of metal wire plasmon is implicitly given in an eigen-value equation. To get the effective index, one

#116803 - $15.00 USD Received 10 Sep 2009; revised 13 Oct 2009; accepted 13 Oct 2009; published 29 Oct 2009

has to use various numerical techniques to solve the related eigen-value equation [5–21]. Therefore, an explicit approximate formula for the effective index is welcome.

In this paper, we shall derive such an approximate explicit formula for metal wire plasmon of terahertz wave. We shall also further test the accuracy and the validity range of the formula. The paper is organized as follows. In Section 2, we shall provide a rough solution to the eigen-value equation and test its accuracy. In the derivation process, the huge relative permittivities of nonmagnetic metals in the spectral region of terahertz wave and some important properties of modified Bessel functions will be used. In Section 3, we shall further transform the rough solution to an approximate solution, and test the accuracy and the validity range of the latter. In the related derivation process, a suitable Taylor expansion and some important properties of the eigen-value equation will be used. And in Section 4, we shall conclude this paper. For simplicity, in this paper, we only discuss the case of nonmagnetic metals whose relative magnetic permeabilities are always 1.

2. A rough solution to the eigen-equation

For a flat metal-dielectric interface, there exists an electromagnetic bound state which is TM polarization, and this bound state is called surface plasmon (SP) [36]. While, in the case of metal wire, SP can also exist at a cylindrical metal-dielectric interface [37,38]. It has one magnetic field component H_φ, and two electric field components E_r and E_z. The only transverse magnetic field component H_φ indicates the TM polarization.

Consider a cylindrical metal wire surrounded by air. We are only interested in axially symmetrical eigenmodes, that is to say, the relations $\partial\mathbf{E}/\partial\varphi = 0$ and $\partial\mathbf{H}/\partial\varphi = 0$ hold in the cylindrical coordinates. For TM polarization of a nonmagnetic metal, by substituting the above-mentioned relations into Maxwell's equations [39] and using the continuities of E_z and H_φ at the interface, one can get the following eigen-equation [5,37,38]:

$$\frac{\varepsilon_m}{\kappa_m}\frac{I_1(k_0\kappa_m R)}{I_0(k_0\kappa_m R)}+\frac{1}{\kappa_a}\frac{K_1(k_0\kappa_a R)}{K_0(k_0\kappa_a R)}=0 \tag{1}$$

where $\kappa_a = [(n_{eff})^2-1]^{1/2}$, $\kappa_m = [(n_{eff})^2-\varepsilon_m]^{1/2}$. n_{eff} is the effective index of the eigenmode, ε_m denotes the relative permittivity of the metal. $I_0(.)$, $K_0(.)$, $I_1(.)$ and $K_1(.)$ are modified Bessel functions. $k_0 = 2\pi/\lambda_0$, where λ_0 and k_0 denotes wavelength and wave number in free space, respectively. R is the radius of the metal wire.

We first consider the first term of Eq. (1). Through a lot of numerical calculations, we find that the effective index n_{eff} is always about 1 provided that the radius R is not extremely small. That is to say, $n_{eff}\approx 1$. On the other hand, the relative permittivity of a metal is huge in the spectral region of THz wave. By taking these two properties into account, one can obtain the following relation.

$$\kappa_m \approx \sqrt{1-\varepsilon_m}. \tag{2}$$

By use of Eq. (2), one can get the following approximation

$$\frac{\varepsilon_m}{\kappa_m}\frac{I_1(k_0\kappa_m R)}{I_0(k_0\kappa_m R)}\approx\frac{\varepsilon_m}{\sqrt{1-\varepsilon_m}}\frac{I_1(k_0R\sqrt{1-\varepsilon_m})}{I_0(k_0R\sqrt{1-\varepsilon_m})}. \tag{3}$$

From Eq. (3) one can find that the first term of Eq. (1) is approximately a constant for a pre-given R. For convenience, we here define this constant as a:

$$a=\frac{\varepsilon_m}{\sqrt{1-\varepsilon_m}}\frac{I_1(k_0R\sqrt{1-\varepsilon_m})}{I_0(k_0R\sqrt{1-\varepsilon_m})}. \tag{4}$$

We now further consider the second term of Eq. (1). Unlike κ_m in the first term, the parameter κ_a in the second term changes apparently with the change of radius R, so does

#116803 - $15.00 USD Received 10 Sep 2009; revised 13 Oct 2009; accepted 13 Oct 2009; published 29 Oct 2009

the ratio $K_1(k_0\kappa_a R)/K_0(k_0\kappa_a R)$. In order to find an approximate expressions for κ_a, we need first to find a suitable approximate for $K_1(k_0\kappa_a R)/K_0(k_0\kappa_a R)$. For convenience, we define the ratio $K_1(k_0\kappa_a R)/K_0(k_0\kappa_a R)$ as a function f(u):

$$f(u) = \frac{K_1(u)}{K_0(u)}, \tag{5}$$

where

$$u = k_0 \kappa_a R. \tag{6}$$

In terms of the parameter a and the function f(u), Eq. (1) can be approximately expressed as

$$a + \frac{f(u)}{\kappa_a} = 0. \tag{7}$$

Equation (7) is the fundament of our further analytical derivation. In other words, our analytical work will be based on Eq. (7).

We denote by $f_r(u)$ a rough expression for f(u). We choose $f_r(u)$ as the following form

$$f_r(u) = 1 + \frac{\alpha}{u}, \tag{8}$$

where α is a constant that needs to be determined. The reasons for such a choice are as follows:

1) By use of the asymptotic properties of modified Bessel functions, one can prove that f (u)~1 + 1/(2u) for very large u. One can further find that both f(u) and $f_r(u)$ approach 1 when u approaches infinity.

2) By use of the asymptotic properties of modified Bessel functions, one can prove that $K_1(u)$~1/u, $K_0(u)$~-ln(u/2) for very small u. However, the change of -ln(u/2) is much slower than that of 1/u. As a result, f(u) approaches infinity basically as the function 1/u does when u is very small. One can find that, except for a coefficient α, both f(u) and $f_r(u)$ approach infinity with the same functional form when u approaches 0.

The constant α can be optimally chosen. Through many numerical tests, we find that u is basically larger than 0.001 when the radius R is larger than the wavelength in the spectral region of terahertz wave. To optimally control the deviation between $f_r(u)$ and f(u) in the wide range from u = 0.001 to u = ∞, we let $f_r(u) = f(u)$ at the point u = 0.01. Accordingly, the coefficient α is determined to be 0.2018. In the remainder of this paper, we shall use the relation

$$\alpha = 0.2018. \tag{9}$$

Both the functions f(u) and $f_r(u)$ in the range of $0.001 \le u \le 10$ are shown in Fig. 1 (a). The corresponding relative deviation $[f(u)-f_r(u)]/f(u)$ is shown in Fig. 1 (b). One can see that the two functions agree well when u approaches 0.01 or u becomes very large. In the range of $0.01 \le u \le 10$, the maximum relative deviation is about 25%. When u is smaller than 0.01, the deviation becomes apparently. In particular, the deviation becomes about 40% at the point u = 0.001. We consider the deviation of about 40% as an acceptable value because $f_r(r)$ is only a rough expression for f(u). Obviously, $f_r(u)$ becomes invalid for smaller u, because the relative deviation becomes larger and larger in this case.

#116803 - $15.00 USD Received 10 Sep 2009; revised 13 Oct 2009; accepted 13 Oct 2009; published 29 Oct 2009

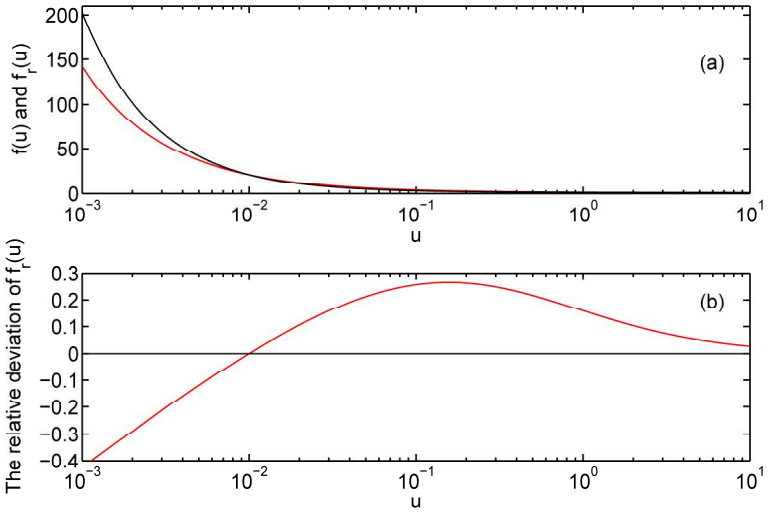

Fig. 1. (a) The comparison between f (u) and f_r (u) in the range of u from 0.001 to 10. The red curve is f(u), and the black curve is $f_r(u)$. (b) The relative deviation between f (u) and f_r (u) in the range of u from 0.001 to 10.

We denote by κ_{ar} a rough expression for κ_a. Replacing the function f(u) and κ_a in Eq. (7) by $f_r(u_r)$ and κ_{ar}, respectively, one can get

$$a + \frac{f_r(u_r)}{\kappa_{ar}} = 0, \tag{10}$$

where

$$u_r = k_0 \kappa_{ar} R. \tag{11}$$

Substituting Eq. (8) and (9) into Eq. (10), one can obtain the following equation

$$a\kappa_{ar}^2 + \kappa_{ar} + c = 0, \tag{12}$$

where

$$c = \frac{0.2018}{k_0 R}. \tag{13}$$

Equation (12) has two roots in mathematics. However, only one of them has physical meaning. Because the field distribution of H_φ decays with the increase of radial coordinate r, κ_{ar} should have a positive real part [5]. Accordingly, one should choose the following root

$$\kappa_{ar} = \frac{-1 - \sqrt{1 - 4ac}}{2a}, \tag{14}$$

where a and c are explicitly given by Eq. (4) and Eq. (13), respectively. The corresponding rough solution n_{effr} for n_{eff} can be further obtained from the relation

$$n_{effr} = \sqrt{\kappa_{ar}^2 + 1}. \tag{15}$$

#116803 - $15.00 USD Received 10 Sep 2009; revised 13 Oct 2009; accepted 13 Oct 2009; published 29 Oct 2009

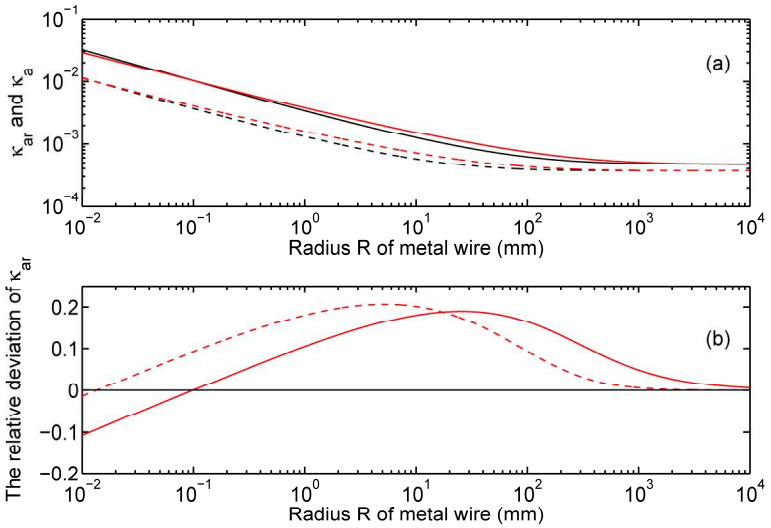

Fig. 2. (a) The comparison between the rough values κar and the exact values κa, for metal copper and 0.5 THz. The red curves are the exact values, and the black curves are the rough solutions. The dashed curves are Im(κ_a) and Im(κ_{ar}), and the solid curves are Re(κ_a) and Re(κ_{ar}). (b) The relative deviation of κar. The solid curve represents the relative deviation of Re(κar), and the dashed curve is the relative deviation of Im(κar).

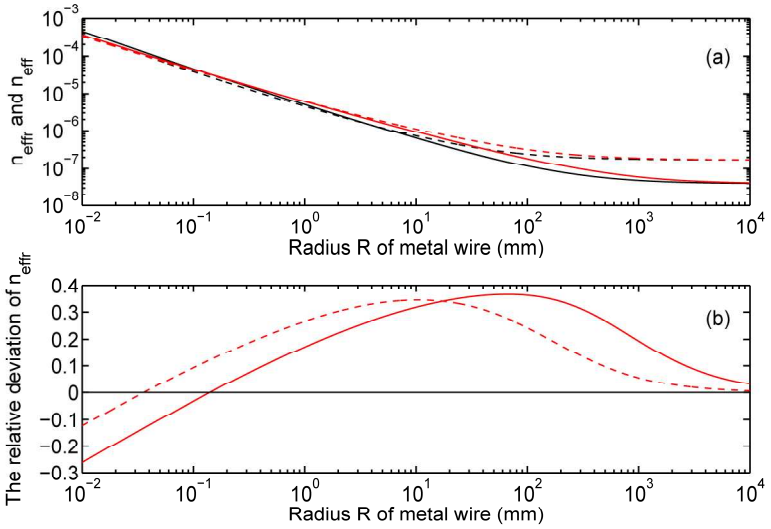

Fig. 3. (a) The comparison between the rough values n_{effr} and the exact values n_{eff}, for metal copper and 0.5 THz. The red curves are the exact values n_{eff}, and the black curves are the rough solutions n_{effr}. The dashed curves are Im(n_{effr}) and Im(n_{eff}), and the solid curves are Re(n_{effr})-1 and Re(n_{eff})-1. (b) The relative deviation of n_{effr}. The solid curve represents the relative deviation of Re(n_{effr})-1, and the dashed curve is the relative deviation of Im(n_{effr}).

To get an intuitive impression on the rough solution, we calculate the κ_{ar} values, as a function of R. The metal is chosen to be copper and the frequency is chosen to be 0.5 THz (i.e., λ_0 = 0.6 mm). The corresponding ε_m value is $\varepsilon_m = -6.3 \times 10^5 + j2.77 \times 10^6$ according to a fitted Drude formula for copper [40]. The scope of metal wire is chosen to

#116803 - $15.00 USD Received 10 Sep 2009; revised 13 Oct 2009; accepted 13 Oct 2009; published 29 Oct 2009

be $0.01\text{mm} \le R \le 10^4\text{mm}$. For comparison, the exact values κ_a are also calculated by numerically solving Eq. (1). The values of κ_{ar} and κ_a are shown in Fig. 2 (a). The relative deviations for the real part and the imaginary part of κ_{ar} are shown in Fig. 2 (b). The rough values n_{effr} and the exact values n_{eff} are shown in Fig. 3 (a). And the relative deviations for the real part and the imaginary part of n_{effr} are shown in Fig. 3 (b).

From the above two figures, we can see that, in the chosen range of $0.01\text{mm} \le R \le 10^4\text{mm}$, the maximum relative deviation of κ_a is about 20%, and the maximum relative deviation of n_{effr} is about 40%. These deviations are rather large. Therefore, the rough solution needs to be further improved.

3. Transform from the rough solution to an approximate solution

In this Section, we shall use a suitable Taylor expansion and the properties of modified Bessel functions to derive an approximate solution with high accuracy. For convenience, we denote by κ_{aa} the approximate expression for κ_a. Then the corresponding approximate expression u_a for u is denoted by

$$u_a = k_0 \kappa_{aa} R. \tag{16}$$

We make the first-order Taylor expansion $f_a(u)$ for the function f(u) at the neighborhood of u_r, which is given by Eq. (11). Accordingly, the value $f_a(u_a)$ at the point u_a can be written as

$$f_a(u_a) = f(u_r) + f'(u_r)(u_a - u_r), \tag{17}$$

where the first-order derivative $f'(u_r)$ is given by

$$f'(u_r) = \frac{K_1^2(u_r)}{K_0^2(u_r)} - \frac{K_1(u_r)}{K_0(u_r)u_r} - 1. \tag{18}$$

Replacing the function f(u) and κ_a in Eq. (7) by $f_a(u_a)$ and κ_{aa}, respectively, one can get

$$a + \frac{f_a(u_a)}{\kappa_{aa}} = 0. \tag{19}$$

Comparing Eq. (19) with Eq. (10), we obtain:

$$\frac{1}{\kappa_{aa}} f_a(u_a) = \frac{1}{\kappa_{ar}} f_r(u_r). \tag{20}$$

Substituting Eq. (17) into Eq. (20), we finally obtain

$$\kappa_{aa} = \kappa_{ar} \frac{f(u_r) - f'(u_r)u_r}{f_r(u_r) - f'(u_r)u_r}, \tag{21}$$

where $f'(u_r)$, u_r, and κ_{ar} are given by Eq. (18), Eq. (11), and Eq. (14), respectively. To this end, we derive an approximately explicit formula for κ_{aa}. The corresponding approximate value n_{effa} for the effective index can be further obtained from the relation

$$n_{effa} = \sqrt{\kappa_{aa}^2 + 1}. \tag{22}$$

To test the validity of the approximate solution, we compare it with the corresponding exact result, which is obtained by numerically solving Eq. (1). The metal, the frequency, and the range of radius are chosen as those in Section 2. The comparisons between the approximate solution κ_{aa} and the exact solution κ_a are shown in Fig. 4. Similarly, the comparisons between the approximate solution n_{effa} and the exact solution n_{eff} are shown in Fig. 5. One can see that, in the chosen range of $0.01\text{mm} \le R \le 10^4\text{mm}$, the

#116803 - $15.00 USD Received 10 Sep 2009; revised 13 Oct 2009; accepted 13 Oct 2009; published 29 Oct 2009

maximum relative deviations of κ_{aa} and of n_{effa} are only about 2% and 3%, respectively. These deviations are much lower than those in the rough solution.

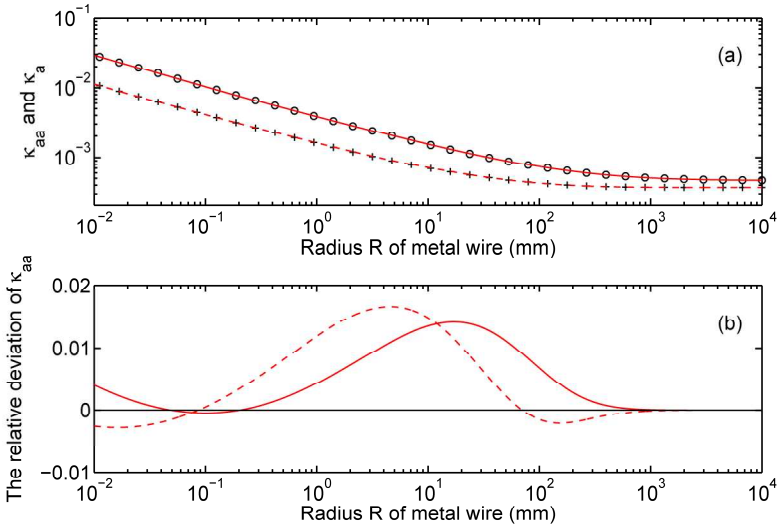

Fig. 4. (a) The comparison between the accurate values κ_{aa} and the exact values κ_a, for metal copper and 0.5 THz. The dashed curve is Im(κ_a) and the signs "+" show Im(κ_{aa}). The solid curve is Re(κ_a) and the signs "o" show Re(κ_{aa}). (b) The relative deviation of κ_{aa}. The solid curve represents the relative deviation of Re(κ_{aa}), and the dashed curve is the relative deviation of Im(κ_{aa}).

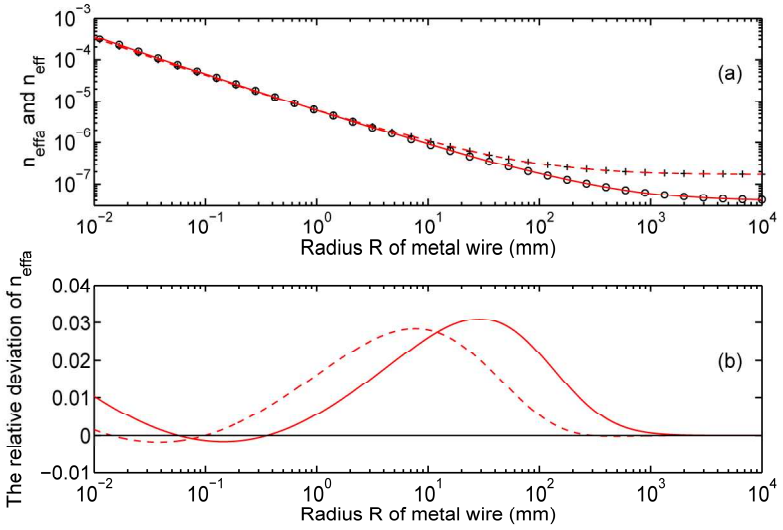

Fig. 5. (a) The comparison between the approximate values n_{effa} and the exact values n_{eff}, for metal copper and 0.5 THz. The dashed curve is Im(n_{eff}) and the signs "+" show Im(n_{effa}). The solid curve is Re (n_{eff})-1 and the signs "o" show Re(n_{effa})-1. (b) The relative deviation of n_{effa}. The solid curve represents the relative deviation of Re(n_{effa})-1, and the dashed curve is the relative deviation of Im(n_{effa}).

In addition, to see whether the approximate solution is valid in the whole range of terahertz radiation, we further make more numerical tests on other bands of THz, especially on the two ends. The results of n_{effa} for copper on 0.1THz and 10THz are

#116803 - $15.00 USD Received 10 Sep 2009; revised 13 Oct 2009; accepted 13 Oct 2009; published 29 Oct 2009

shown Fig. 6 and Fig. 7. From them, we can see that the approximate solution performs well in the whole range of terahertz radiation, especially on the higher frequency. The reason is that a higher frequency leads to a larger absolute value of u and better results.

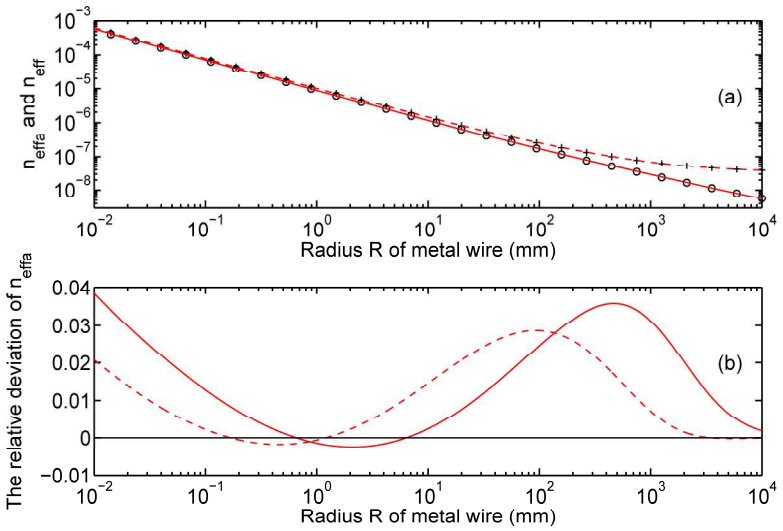

Fig. 6. The comparison between the approximate values n_{effa} and the exact values n_{eff}, for metal copper and 0.1 THz. The dashed curve is Im(n_{eff}) and the signs "+" show Im(n_{effa}). The solid curve is Re(n_{eff})-1 and the signs "o" show Re(n_{effa})-1. (b) The relative deviation of n_{effa}. The solid curve represents the relative deviation of Re(n_{effa})-1, and the dashed curve is the relative deviation of Im(n_{effa}).

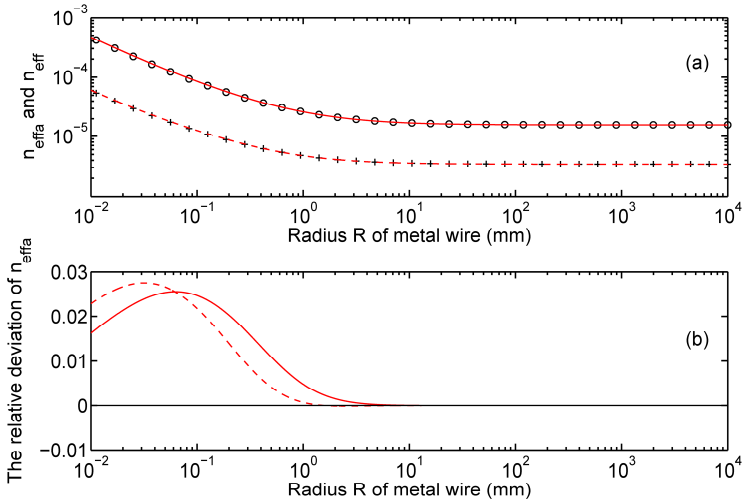

Fig. 7. The comparison between the approximate values n_{effa} and the exact values n_{eff}, for metal copper and 10 THz. The dashed curve is Im(n_{eff}) and the signs "+" show Im(n_{effa}), and the solid curve is Re(n_{effa})-1 and the signs "o" show Re(n_{eff})-1. (b) The relative deviation of n_{effa}. The solid curve represents the relative deviation of Re(n_{effa})-1, and the dashed curve is the relative deviation of Im(n_{effa}).

To further test the applicability of our formula on more metals, we make numerical tests on other nonmagnetic metals mentioned in Ref [33]. We find that our formula performs also well for all other nonmagnetic metals of Al, Ag, Au, Mo, W, Pd, Ti, Pb,

#116803 - $15.00 USD Received 10 Sep 2009; revised 13 Oct 2009; accepted 13 Oct 2009; published 29 Oct 2009

Pt, V. The maximum relative deviation of the effective index for all 11 tested nonmagnetic metals is smaller than 5% in the whole spectral region of THz wave when the radius of metal wire is in the wide range from 10μm to 10^4 mm. We do not test the magnetic metals of Co, Fe and Ni because they are beyond the scope of this paper.

It should be pointed out that the approximate solution is actually valid for the wide radius range from 10μm to infinity, though its validity is only directly shown for the radius range of $10\mu m \le R \le 10^4$ mm in Figs. 2-7. In each case, the accuracy of the approximate solution at a radius larger than 10^4 mm is higher than that at the radius of 10^4 mm.

4. Conclusions

In conclusion, we have obtained an explicit formula for metal wire plasmon of terahertz wave. This formula is valid for all the tested 11 kinds of nonmagnetic metals, for the whole spectral region of terahertz wave, and for the wide radius range from 10μm to infinity. For all the numerical tests, the relative deviation of the approximate formula for the effective index is smaller than 5%. The obtained formula can be used for the fast analyses and designs of metal wire plasmon of terahertz wave.

#116803 - $15.00 USD Received 10 Sep 2009; revised 13 Oct 2009; accepted 13 Oct 2009; published 29 Oct 2009